Generation of electromagnetic waves from 0.3 to 1.6 terahertz with a high-T_c superconducting $Bi_2Sr_2CaCu_2O_{8+\delta}$ intrinsic Josephson junction emitter

Takanari Kashiwagi,[1,2] Takashi Yamamoto,[3] Takeo Kitamura,[1] Kentaro Asanuma,[1] Chiharu Watanabe,[1] Kurama Nakade,[1] Takaki Yasui,[1] Yoshihiko Saiwai,[1] Yuuki Shibano,[1] Hiroyuki Kubo,[4] Kazuki Sakamoto,[4] Takuya Katsuragawa,[4] Manabu Tsujimoto,[5] Kaveh Delfanazari,[6] Ryozo Yoshizaki,[1,2] Hidetoshi Minami,[1,2] Richard A. Klemm,[7] and Kazuo Kadowaki[1,2]

[1]*Graduate School of Pure and Applied Sciences, University of Tsukuba, 1-1-1 Tennodai, Tsukuba, Japan*
[2]*Division of Materials Science, Faculty of Pure and Applied Sciences, University of Tsukuba, 1-1-1, Tennodai, Tsukuba, Ibaraki 305-8573, Japan*
[3]*Wide Bandgap Materials Group, Optical and Electronic Materials Unit, Environment and Energy Materials Division, National Institute for Materials Science, 1-1 Namiki, Tsukuba, Ibaraki 305-0044, Japan*
[4]*College of Engineering Sciences, University of Tsukuba, 1-1-1 Tennodai, Tsukuba, Japan*
[5]*Department of Electronic Science and Engineering, Kyoto University, Nishikyo-ku, Kyoto 615-8510, Japan*
[6]*Optoelectronics Research Centre and Centre for Photonic Metamaterials, University of Southampton, Highfield, Southampton SO17 1BJ, United Kingdom*
[7]*Department of Physics, University of Central Florida, 4000 Central Florida Blvd., Orlando, Florida 32816-2385, USA*

(Received 23 January 2015; accepted 23 February 2015; published online 4 March 2015)

To obtain higher power P and frequency f emissions from the intrinsic Josephson junctions in a high-T_c superconducting $Bi_2Sr_2CaCu_2O_{8+\delta}$ single crystal, we embedded a rectangular stand-alone mesa of that material in a sandwich structure to allow for efficient heat exhaust. By varying the current-voltage (I-V) bias conditions and the bath temperature T_b, f is tunable from 0.3 to 1.6 THz. The maximum P of a few tens of μW, an order of magnitude greater than from previous devices, was found at $T_b \sim 55$ K on an inner I-V branch at the TM(1,0) cavity resonance mode frequency. The highest f of 1.6 THz was found at $T_b = 10$ K on an inner I–V branch, but away from cavity resonance frequencies. A possible explanation is presented. © *2015 AIP Publishing LLC*.
[http://dx.doi.org/10.1063/1.4914083]

The intrinsic Josephson junction (IJJ) terahertz (THz) emitter (IJJ-THz emitter) based on the IJJs present in the high-T_c superconductor $Bi_2Sr_2CaCu_2O_{8+\delta}$ (Bi2212)[1–3] has been developed experimentally[4–31] and theoretically.[32–46] So far, its demonstrated radiation characteristics are the f range from 0.3 to 1.0 THz,[4,22,23] the maximum P of $\sim$30 μW,[19–22] and coherent, continuous-wave emission with a spectral width of less than 0.5 GHz.[12,13] Recently, by synchronizing the emissions from a three-mesa array, $P \sim 610$ μW was reported.[17] Using these characteristic features, THz imaging systems[29–31] and THz emission and detection system both based on high-T_c superconductors[19] are also developed. These THz technologies using IJJs are compatible with the recently developed semiconductor THz devices such as the resonant tunneling diodes[47,48] and the quantum cascade lasers.[49–51] The characteristic features of the IJJ-THz emitter were recently reviewed.[52]

An important issue for high P generation from the IJJ-THz emitter is how to minimize the Joule heating effects due to the dc bias current I. From the low temperature scanning laser microscopy technique,[5–7] the direct temperature distribution $T(\mathbf{r})$ measurements of mesas by using photoluminescence techniques,[24–27] and the numerical simulations,[43,44] the Joule heating was often found to cause severely inhomogeneous $T(\mathbf{r})$ in the mesa, including hot spots with $T(\mathbf{r}) > T_c$, greatly reducing P. Such heating effects reduce the hysteresis area of the current-voltage (I-V) characteristics (IVCs), and lead to a discontinuous drop in V in the lower I bias region of the outer IVC branch.

For the earliest mesas with substrates formed from the same Bi2212 crystal, the emission intensity observed nearly parallel to the substrate was vanishingly small,[10] and it was proposed that replacing the Bi2212 substrate with an insulating—or preferably, a normal conducting—one might potentially increase the overall output P by more than two orders of magnitude.[40,41] This led to studies of stand-alone mesas, or *mesas without a superconducting substrate*, which had instead Au layers both on top and beneath the Bi2212 mesa. The observed emission P from stand-alone mesas was at least one order of magnitude higher than from mesas with Bi2212 substrates.[19,21,22] Here, we describe a simple device structure based on the stand-alone mesa that is easy to fabricate, assemble, and operate, and produces highly reproducible high-power emission that is tunable from 0.3 to 1.6 THz.

To make stand-alone mesas, we used high-quality single crystals of Bi2212 grown by a traveling-solvent floating-zone method using a modified infrared image furnace.[53,54] We first annealed a piece of a Bi2212 single crystal overnight to obtain an appropriate doping level.[10–12,20–22] After freshly cleaving both surfaces of a piece of the annealed Bi2212 single crystal, making it a few μm thick, both surfaces were coated with silver and gold by evaporation.

Several rectangular stand-alone mesas 350 μm in length, 58–66 μm in width (top-bottom), and 4.7 μm in thickness, including the electrode pads of the Ag and Au layers, were fabricated by Ar ion milling using different metallic masks to define the length and the width of each mesa.[14] $T_c \sim 76$ K

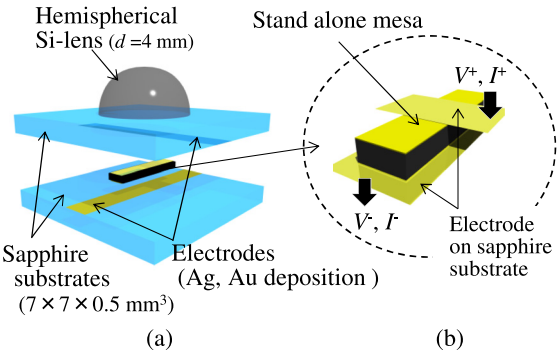

FIG. 1. (a) Sketches of (a) a stand-alone mesa sandwiched by two sapphire substrates and (b) its electrical contacts.

was measured resistively, and the thickness was estimated with a scanning electron microscope.

Figure 1(a) is a sketch of the stand-alone mesa device. The stand-alone mesa was sandwiched between identical sapphire substrates of dimensions $7.0 \times 7.0 \times 0.5\,\text{mm}^3$, in order to efficiently remove the Joule heat generated by I. Prior to the sandwich construction, long rectangular electrode layers of Ag and then Au about 50–100 nm in thicknesses and 100 μm in widths were deposited on each sapphire substrate, and the top and bottom sapphire Au electrodes were arranged to meet the top and bottom stand-alone mesa Au surfaces face-to-face in a perpendicular fashion, as sketched in Figs. 1(a) and 1(b). After the sandwich structure was assembled, it was gently pressed by four screws mounted at the corners of the device. A hemispherical Si-lens 4 mm in diameter was attached onto a sapphire plate for emission focusing, as shown in Fig. 1(a). Full details of the stand-alone mesa sandwich device fabrication will be described elsewhere.

Figure 2(a) shows typical outer-branch IVCs of the stand-alone mesa sandwich device at bath temperatures $T_b = 15$ K, 50 K, and 70 K. The contact resistance was subtracted from the data. It is remarkable that at 15 K, the bias V is as high as 7 V even though the mesa is 3–4 times thicker than those previously studied.[10–12] Furthermore, neither IVC back-bending nor clear IVC jumps at low T_b values were found. Since those features were previously associated with mesa overheating and possibly with hot-spot formation, the present IVCs suggest improved heat removal efficiency of this device.

The observed radiation intensities from the stand-alone mesa sandwich device detected by the InSb hot-electron (HE) bolometer are displayed in Fig. 2(a) by the circle sizes and colors on the IVCs. The intensity shows a maximum around $T_b = 55$ K, as observed previously.[20,22] Using the power meter (VDI Erickson PM4), we also directly measured the maximum radiation power P at 56 K to be $\sim$6.5 μW at the $V \sim 2.2$ V bias point. Accounting for the rectangular mesa radiation pattern and the losses at the detector and from all materials between the mesa and the detector, the total radiation power was estimated to be on the order of a few tens of μW, comparable to the maximum power observed from previous stand-alone mesas.[19,21,22]

In Fig. 2(b), f is plotted versus the bias V at the color-coded T_b values. The f data were mostly obtained from the outer-most IVC branches. f is highly T_b-dependent, with higher f values observed at lower T_b to lower f values seen at higher T_b. Thus, remarkably very broad f tunability can be obtained continuously for this device by varying T_b and V. The maximum $f = 1.15$ THz from outer branches was detected at $T_b = 13$ K, whereas the lowest $f = 0.29$ THz was observed at $T_b = 71$ K. Similar behavior was reported previously.[6,8,22,23]

Most of the experimental data shown in Fig. 2(b) follow the ac-Josephson relation, $f = f_J = 2eV/(N_{act}h)$, where e is the electronic charge, h is Planck's constant, and N_{act} is the number of IJJs active in the emission. The dotted line is a fit to the ac-Josephson relation with $N_{fit} = 2719$, which is slightly lower than the total number $N \sim 3100$ of mesa IJJs estimated from 4.7 μm and 1.533 nm for the respective mesa and IJJ thicknesses.

The large T_b dependence of f is just a consequence of the T_b-dependent change of the bias V while fixing the ac Josephson relation, as long as the number N_{act} of emitting IJJs is independent of T_b. Note that there are points deviating from the dotted line, especially around $f \approx 0.6$ THz. These non-conforming data points arise from the inner IVC

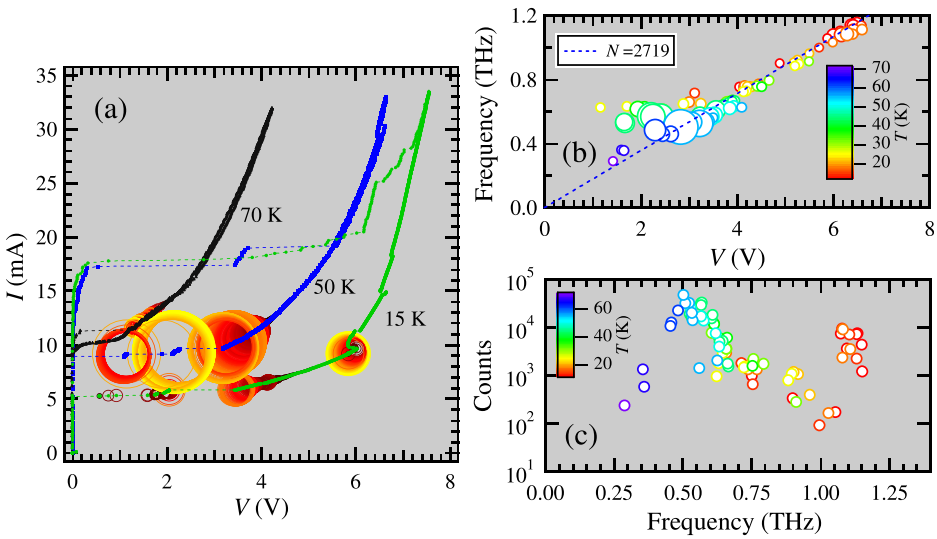

FIG. 2. (a) Typical IVCs at $T_b = 15$ K, 50 K, and 70 K of the stand-alone mesa sandwich device. Circle sizes and colors indicate the radiation intensities detected by the InSb HE bolometer. (b) The observed radiation f versus applied bias V of the device at the color-coded T_b values. Circle sizes indicate the spectral radiation intensities detected by the FT-IR spectrometer. The dotted line is a linear fit of the ac-Josephson relation to the data for $N_{fit} = 2719$ IJJs. (c) Logarithmic spectral radiation intensity versus f detected by the FT-IR spectrometer at the color-coded T_b values.

branches with smaller N_{act} values, not on the outer-most IVC branch, for which $N_{act} \approx N \sim 3100$ is fixed to be all of the IJJs in the device.[11]

The spectral intensities measured by the FT-IR spectrometer for the data in Fig. 2(b) are logarithmically plotted versus f in Fig. 2(c). The radiation intensity spectrum has distinct peaks at around 0.55 THz and 1.1 THz, which fall within the respective TM(1,0) and T(2,0) cavity resonance mode frequency ranges ($0.62 \sim 0.54$ THz and $1.2 \sim 1.1$ THz) of the rectangular mesa of width range 58–66 μm and index of refraction $n \sim 4.2$.[10–12,20–22] This strongly suggests that both of these cavity resonance modes are enhancing the output P. These two modes were also seen in Fig. 2(a), where the TM(1,0) mode is excited at around 2.2 V at 50 K, and the TM(2,0) mode is excited at 6 V at 15 K. The P observed at the lower TM(1,0) mode frequency and higher T_b values is an order of magnitude stronger than that observed at the higher TM(2,0) mode frequency and lower T_b values. The emission P from the TM(1,0) mode excitation has a maximum at 55 K, sharply decreases with further increase in T_b, and fades away around 65 K.

To obtain further information about the relation between the emission P and f, we measured the radiation properties of the inner-branch IVCs. These are plotted in Figs. 3(a) and 3(b) at $T_b = 10$ K and 55 K, respectively. The black dots represent the IVC points. The measured f points are denoted by the white filled circles. From these two f data sets, color-coded contour plots of f are mapped onto the multi-branch IVC structures.

As seen in Figs. 3(a) and 3(b), at fixed T_b, the radiation f increases strongly with bias I at fixed V and weakly with decreasing bias V at fixed I. From the ac Josephson relation, $f \propto V/N_{act}$, increasing f and I at fixed V clearly implies decreasing N_{act}. Due to the positively sloped IVC branches, decreasing V at fixed I also leads to a decrease in N_{act} and increasing radiation f values. Both the f tunability and IVC plot ranges observed here are much wider than in the similar behavior observed previously,[11] perhaps due to the more efficient Joule heat removal of our present stand-alone mesa sandwich structure and to the much thicker present mesa.

In Fig. 4, we display more details of the multi-branch IVC emission behavior at 10 K and 55 K. As shown in Figs. 4(a) and 4(e), the observed radiation frequencies $f \propto V$ in each branch, in agreement with the ac Josephson relation and with a previous report,[11] and very wide f ranges were seen. At $T_b = 10$ K, f ranges from about 0.69 THz to 1.63 THz in the multi-branching IVCs.

The radiation spectra from a nearly outer-most IVC branch at $T_b = 10$ K are displayed in Fig. 4(c). These data clearly show a strong enhancement of the radiation intensity around 1.1 THz. The strongest radiation on this branch was observed at $f \sim 1.14$ THz, corresponding to the TM(2,0) mode, at the bias $V \sim 6.3$ V.

The record high radiation $f = f_{max} = 1.63$ THz was observed on an inner branch at the bias $V \sim 4$ V, as displayed in Figs. 4(a) and 4(d). This value is the highest frequency so far detected from any IJJ device. The radiation intensity spectra observed in the vicinity ($1.35 \sim 1.63$ THz and $V \sim 4$ V) of f_{max} are displayed in Fig. 4(d). As f increases, the intensity decreases and its spectrum appears to split, as highlighted by the black-arrow eye guides. This may suggest that the emission from the entire mesa is not completely synchronized in this higher f range. We note that f in this range does not match a predicted cavity mode frequency.

On the other hand, at the higher $T_b = 55$ K, radiation f values ranging from ~0.42 THz to 0.69 THz were observed on the inner IVC branches, as shown in Figs. 4(e)–4(g). The observed radiation mostly satisfies $f \propto V$, as at $T_b = 10$ K, but a clear deviation from linearity was also observed in the higher f region. This may be due to self-heating effects at higher I biases, resulting in non-uniform mesa potential conditions. The strongest radiation in this mesa was observed at $f = 0.50$ THz within the very narrow V and I bias ranges around ~2.0 V and 12 mA in some inner IVC branches, as seen in Figs. 4(e) and 4(g), where the TM(1,0) geometrical cavity mode resonance enhancement mechanism appears to be robust. We note that the peak frequency of 0.50 THz is slightly lower than that range ($0.62 \sim 0.54$ THz) expected from the TM(1,0) mode for the mesa width range (58–66 μm). According to patch antenna theory,[55,56] this could arise from mesa fringing effects, which increase in importance with mesa thickness. Accounting for such fringing effects, the revised expected radiation f range is $0.58 \sim 0.51$ THz, much closer to the observed 0.50 THz.

Finally, we would like to emphasize two points. First, as shown in Figs. 2(a), 3(a), and 3(b), the IVCs obtained from this device construction do not exhibit any clear back bending. Since IVC back bending is symptomatic of

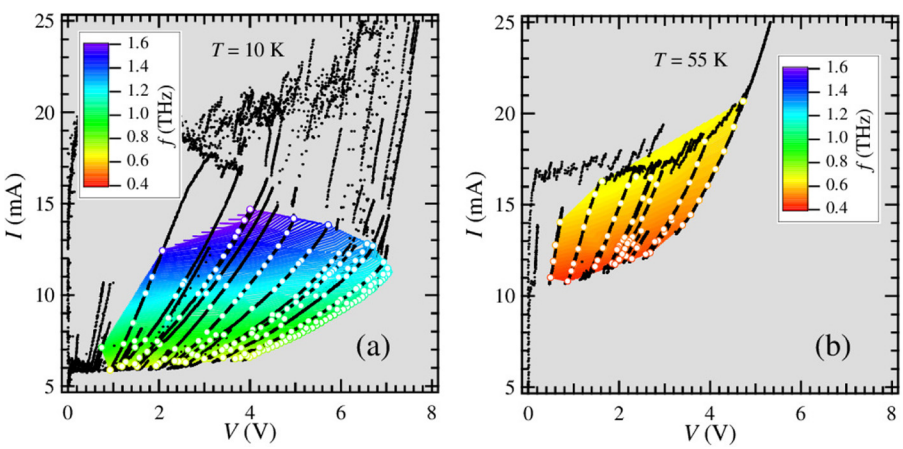

FIG. 3. Black dots: Multi-branching IVCs of the stand-alone mesa sandwich device at (a) $T_b = 10$ K and (b) $T_b = 55$ K. Filled white circles: Bias points where the color-coded radiation f was measured by the FT-IR spectrometer.

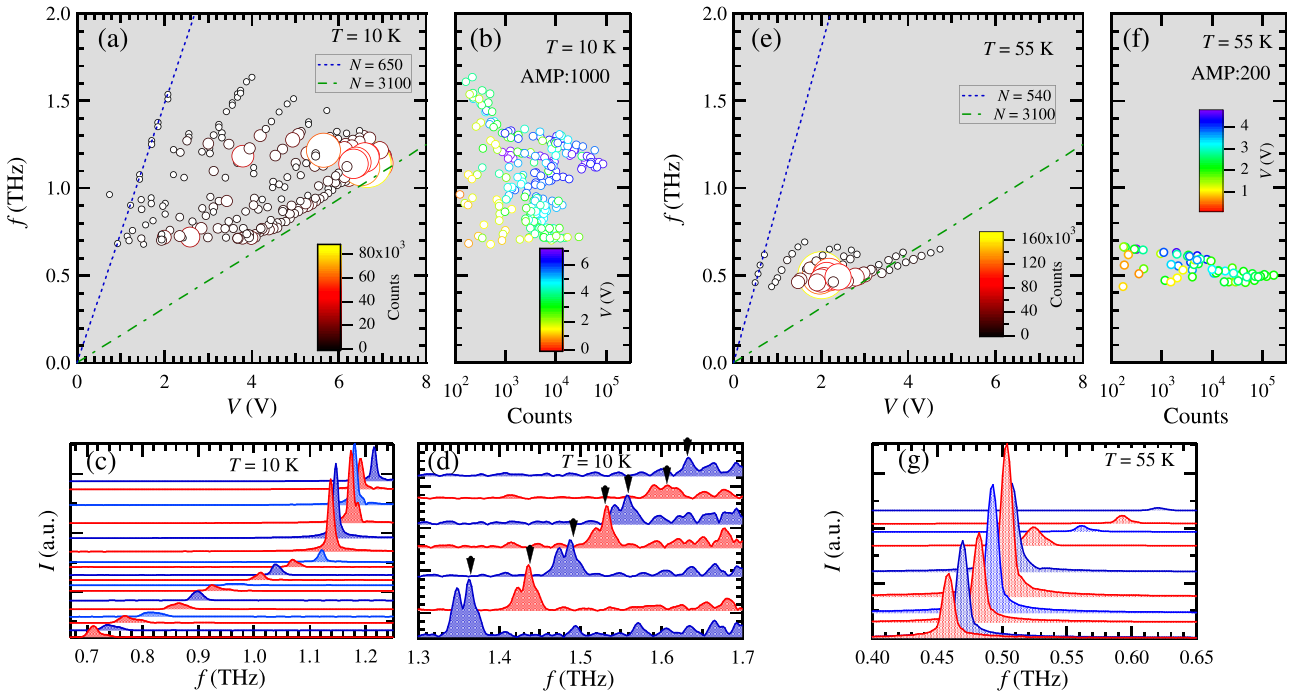

FIG. 4. (a) Plot of the multiple IVC branch radiation f detected by the FT-IR spectrometer versus the applied bias V at $T_b = 10$ K. Symbol sizes and the color code describe the radiation intensity. The blue and green lines are ac Josephson relation fits. (b) Plot of the multiple IVC branch spectral radiation intensity distribution versus f at 10 K in a semi-logarithmic plot. (c) The radiation intensity spectra observed from a nearly outer-most IVC branch at 10 K. (d) The spectra observed from the inner IVC branches at $V \sim 4$ V. The black arrows are eye guides. (e) and (f) correspond to (a) and (b) at $T_b = 55$ K, respectively. (g) The intensity spectra observed in the inner emitting IVC branches at 55 K. The respective detector amplifier gains in (b) and (f) are 1000 and 200.

overheating and hot-spot formation, it appears that the present mesa device might not exhibit any hot spots in the IVC and T_b ranges studied. Furthermore, because of the lack of clear back-bending behavior, the bias V can be increased to ≥ 7.0 V, corresponding to ~ 2.2 mV per IJJ. This higher V/N ratio for the thicker present mesa device was allowed by its more efficient cooling mechanism. Hence, the present device structure may allow for further increases in f beyond the present $f_{max} = 1.6$ THz.

Second, the strongest radiation was observed from a particular inner IVC branch among many other branches at 55 K, as shown in Fig. 4(e). This suggests that this particular IVC branch may provide the optimal number N_{act} of active junctions for the overall emission synchronization, although the larger number N of IJJs would enhance the radiation intensity. These numbers appear to be strongly constrained both by the ac Josephson effect and by the cavity resonance condition. In addition, another stand-alone mesa was recently reported to exhibit characteristic step structures in the bias V at the IVC points of strongest radiation intensity.[22] The step structures suggest that at the cavity resonance condition points, the mesa may self organize so as to optimize the radiation properties. This self-organized radiation optimization supports our above observation regarding a possible emission synchronization mechanism clue, and could be important for further study to better understand the mechanism of THz radiation phenomena.

T.K. was supported by a research grant from The Mazda Foundation and a JST A-step grant. We thank the staff members of the Central Workshop at the University of Tsukuba for machining support.

[1]R. Kleiner, F. Steinmeyer, G. Kunkel, and P. Müller, Phys. Rev. Lett. **68**, 2394 (1992).
[2]R. Kleiner and P. Müller, Phys. Rev. B **49**, 1327 (1994).
[3]A. A. Yurgens, Supercond. Sci. Technol. **13**, R85 (2000).
[4]L. Ozyuzer, A. E. Koshelev, C. Kurter, N. Gopalsami, Q. Li, M. Tachiki, K. Kadowaki, T. Yamamoto, H. Minami, H. Yamaguchi *et al.*, Science **318**, 1291 (2007).
[5]H. B. Wang, S. Guénon, J. Yuan, A. Iishi, S. Arisawa, T. Hatano, T. Yamashita, D. Koelle, and R. Kleiner, Phys. Rev. Lett. **102**, 017006 (2009).
[6]H. B. Wang, S. Guénon, B. Gross, J. Yuan, Z. G. Jiang, Y. Y. Zhong, M. Grünzweig, A. Iishi, P. H. Wu, T. Hatano, D. Koelle, and R. Kleiner, Phys. Rev. Lett. **105**, 057002 (2010).
[7]S. Guénon, M. Grünzweig, B. Gross, J. Yuan, Z. G. Jiang, Y. Y. Zhong, M. Y. Li, A. Iishi, P. H. Wu, T. Hatano *et al.*, Phys. Rev. B **82**, 214506 (2010).
[8]T. M. Benseman, A. E. Koshelev, K. E. Gray, W.-K. Kwok, U. Welp, K. Kadowaki, M. Tachiki, and T. Yamamoto, Phys. Rev. B **84**, 064523 (2011).
[9]H. Koseoglu, F. Turkoglu, Y. Simsek, and L. Ozyuzer, J. Supercond. Novel Magn. **24**, 1083 (2011).
[10]K. Kadowaki, M. Tsujimoto, K. Yamaki, T. Yamamoto, T. Kashiwagi, H. Minami, M. Tachiki, and R. A. Klemm, J. Phys. Soc. Jpn. **79**, 023703 (2010).
[11]M. Tsujimoto, T. Yamamoto, K. Delfanazari, R. Nakayama, T. Kitamura, M. Sawamura, T. Kashiwagi, H. Minami, M. Tachiki, K. Kadowaki, and R. A. Klemm, Phys. Rev. Lett. **108**, 107006 (2012).
[12]T. Kashiwagi, M. Tsujimoto, T. Yamamoto, H. Minami, K. Yamaki, K. Delfanazari, K. Deguchi, N. Orita, T. Koike, R. Nakayama *et al.*, Jpn. J. Appl. Phys. **51**, 010113 (2012).
[13]M. Li, J. Yuan, N. Kinev, J. Li, B. Gross, S. Guenon, A. Ishii, K. Hirata, T. Hatano, D. Koelle *et al.*, Phys. Rev. B **86**, 060505 (2012).
[14]H. Minami, M. Tsujimoto, T. Kashiwagi, T. Yamamoto, and K. Kadowaki, IEICE Trans. Electron. **E95-C**, 347 (2012).
[15]I. Kakeya, Y. Omukai, T. Yamamoto, K. Kadowaki, and M. Suzuki, Appl. Phys. Lett. **100**, 242603 (2012).
[16]F. Turkoglu, H. Koseoglu, Y. Demirhan, L. Ozyuzer, S. Preu, S. Malzer, Y. Simsek, P. Müller, T. Yamamoto, and K. Kadowaki, Supercond. Sci. Technol. **25**, 125004 (2012).
[17]T. M. Benseman, K. E. Gray, A. E. Koshelev, W.-K. Kwok, U. Welp, H. Minami, K. Kadowaki, and T. Yamamoto, Appl. Phys. Lett. **103**, 022602 (2013).

[18]J. Yuan, M. Y. Li, J. Li, B. Gross, A. Ishii, K. Yamaura, T. Hatano, K. Hirata, E. Takayama-Muromachi, P. H. Wu *et al.*, Supercond. Sci. Technol. **25**, 075015 (2012).
[19]D. Y. An, J. Yuan, N. Kinev, M. Y. Li, Y. Huang, M. Ji, H. Zhang, Z. L. Sun, L. Kang, B. B. Jin *et al.*, Appl. Phys. Lett. **102**, 092601 (2013).
[20]S. Sekimoto, C. Watanabe, H. Minami, T. Yamamoto, T. Kashiwagi, R. A. Klemm, and K. Kadowaki, Appl. Phys. Lett. **103**, 182601 (2013).
[21]K. Kadowaki, M. Tsujimoto, K. Delfanazari, T. Kitamura, M. Sawamura, H. Asai, T. Yamamoto, K. Ishida, C. Watanabe, S. Sekimoto *et al.*, Physica C **491**, 2 (2013).
[22]T. Kitamura, T. Kashiwagi, T. Yamamoto, M. Tsujimoto, C. Watanabe, K. Ishida, S. Sekimoto, K. Asanuma, T. Yasui, K. Nakade *et al.*, Appl. Phys. Lett. **105**, 202603 (2014).
[23]M. Ji, J. Yuan, B. Gross, F. Rudau, D. Y. An, M. Y. Li, X. J. Zhou, Y. Huang, H. C. Sun, Q. Zhu *et al.*, Appl. Phys. Lett. **105**, 122602 (2014).
[24]S. Niratisairak, Ø. Haugen, T. H. Johansen, and T. Ishibashi, Physica C **468**, 442 (2008).
[25]T. M. Benseman, A. E. Koshelev, W.-K. Kwok, U. Welp, V. K. Vlasko-Vlasov, K. Kadowaki, H. Minami, and C. Watanabe, J. Appl. Phys. **113**, 133902 (2013).
[26]H. Minami, C. Watanabe, K. Sato, S. Sekimoto, T. Yamamoto, T. Kashiwagi, R. A. Klemm, and K. Kadowaki, Phys. Rev. B **89**, 054503 (2014).
[27]C. Watanabe, H. Minami, S. Sekimoto, T. Yamamoto, T. Kashiwagi, R. A. Klemm, and K. Kadowaki, J. Phys.: Condens. Matter **26**, 172201 (2014).
[28]M. Tsujimoto, H. Kambara, Y. Maeda, Y. Yoshioka, Y. Nakagawa, and I. Kakeya, Phys. Rev. Appl. **2**, 044016 (2014).
[29]M. Tsujimoto, H. Minami, K. Delfanazari, M. Sawamura, R. Nakayama, T. Kitamura, T. Yamamoto, T. Kashiwagi, T. Hattori, and K. Kadowaki, J. Appl. Phys. **111**, 123111 (2012).
[30]T. Kashiwagi, K. Nakade, B. Markovic, Y. Saiwai, H. Minami, T. Kitamura, C. Watanabe, K. Ishida, S. Sekimoto, K. Asanuma *et al.*, Appl. Phys. Lett. **104**, 022601 (2014).
[31]T. Kashiwagi, K. Nakade, Y. Saiwai, H. Minami, T. Kitamura, C. Watanabe, K. Ishida, S. Sekimoto, K. Asanuma, T. Yasui *et al.*, Appl. Phys. Lett. **104**, 082603 (2014).
[32]L. N. Bulaevskii and A. E. Koshelev, Phys. Rev. Lett. **99**, 057002 (2007).
[33]S. Lin and X. Hu, Phys. Rev. Lett. **100**, 247006 (2008).
[34]X. Hu and S. Lin, Phys. Rev. B **78**, 134510 (2008).
[35]A. E. Koshelev and L. N. Bulaevskii, Phys. Rev. B **77**, 014530 (2008).
[36]A. E. Koshelev, Phys. Rev. B **78**, 174509 (2008).
[37]M. Tachiki, S. Fukuya, and T. Koyama, Phys. Rev. Lett. **102**, 127002 (2009).
[38]M. Machida, Y. Ota, N. Sasa, T. Koyama, and H. Matsumoto, J. Phys. Conf. Ser. **248**, 012037 (2010).
[39]A. E. Koshelev, Phys. Rev. B **82**, 174512 (2010).
[40]R. A. Klemm and K. Kadowaki, J. Supercond. Novel Magn. **23**, 613 (2010).
[41]R. A. Klemm and K. Kadowaki, J. Phys.: Condens. Matter **22**, 375701 (2010).
[42]V. M. Krasnov, Phys. Rev. B **83**, 174517 (2011).
[43]A. A. Yurgens, Phys. Rev. B **83**, 184501 (2011).
[44]B. Gross, S. Guénon, J. Yuan, M. Y. Li, J. Li, A. Ishii, R. G. Mints, T. Hatano, P. H. Wu, D. Koelle, H. B. Wang, and R. Kleiner, Phys. Rev. B **86**, 094524 (2012).
[45]S. Lin and X. Hu, Phys. Rev. B **86**, 054506 (2012).
[46]H. Asai and S. Kawabata, Appl. Phys. Lett. **104**, 112601 (2014).
[47]Y. Koyama, R. Sekiguchi, and T. Ouchi, APEX **6**, 064102 (2013).
[48]H. Kanaya, R. Sogabe, T. Maekawa, S. Suzuki, and M. Asada, J. Infrared Millimeter Terahertz Waves **35**, 425 (2014).
[49]C. Walther, M. Fischer, G. Scalari, R. Terazzi, N. Hoyler, and J. Faist, Appl. Phys. Lett. **91**, 131122 (2007).
[50]S. Fathololoumi, E. Dupont, C. W. I. Chan, Z. R. Wasilewski, S. R. Laframboise, D. Ban, A. Mátyás, C. Jirauschek, Q. Hu, and H. C. Liu, Opt. Express **20**, 3866 (2012).
[51]J. Kiessling, I. Breunig, P. G. Schunemann, K. Buse, and K. Vodopyanov, New J. Phys. **15**, 105014 (2013).
[52]U. Welp, K. Kadowaki, and R. Kleiner, Nat. Photonics **7**, 702 (2013).
[53]T. Mochiku and K. Kadowaki, Physica C **235–240**, 523 (1994).
[54]T. Mochiku, K. Hirata, and K. Kadowaki, Physica C **282–287**, 475 (1997).
[55]J. R. James, P. S. Hall, and C. Wood, *Microstrip Antenna Theory and Design*, IEE Electromagnetic Waves Series Vol. 12 (IEEE Press, New York, 1981).
[56]M. Haneishi, K. Hirasawa, and S. Suzuki, *Small and Planar Antennas* (Coronasha, Tokyo, 1996) [in Japanese].